Personal Statement

Research Experience

As an undergraduate at the University of Central Florida (UCF) I worked for Joe Harrington for four years and earned BS degrees in Math and Physics. Joe's group studies exoplanets using transit, secondary eclipse, and radial velocity data.

My first year working with Joe, I used the group's orbits code (rv, Campo et al. 2011) which fits orbital parameters to data from stellar radial velocity measurements and transit and secondary eclipse timing using a Markov chain. I used this code to fit an orbit to the planet TrES-1b (Cubillos et al. 2014).

During my second and third years of working for Joe, I worked on a code called Bayesian Atmospheric Radiative Transfer (BART, Harrington et al. 2019). BART uses a Markov chain to constrain the atmospheres of hot-Jupiter exoplanets by fitting the radiative transfer model described by Rojo (2006) to transit and secondary eclipse spectroscopy data.

I optimized the radiative transfer model so it could run 10^5 to 10^7 times within the Markov chain. Patricio Cubillos and I went through all 15,000+ lines of code to determine what could be moved to an initialization function which would be run first, and what would have to be looped over for every iteration. After that, we used a code performance profiler to further optimize the runtime of the code.

During my third rnd fourth years of working for Joe, I used our Photometry for Orbits, Eclipses, and Transits (POET, Stevenson et al. (2012)) pipeline to fit a light curve to two secondary-eclipse observations of the planet HAT-P-30b. A companion star complicated this analysis, and I modified POET to be able to model and subtract out the flux from this companion star. I then used our orbit code to fit an orbit to HAT-P-30b. Finally, I used BART to fit an atmosphere to HAT-P-30b and published a first-author paper. (Foster et al. 2019).

Outreach and Education Experience

At UCF, I ran the Astronomy Society. We held an open-to-the-public observing event every week (weather permitting) at the UCF Robinson Observatory 8-inch telescopes on the lawn and a tour inside of the observatory and its half-meter telescope. We would give additional private events for groups such as scout troops or local elementary schools in exchange for donations for our annual science project, a stratospheric weather balloon launch.

In grad school at Cornell, I am the outreach coordinator for the graduate students, organizing events at local libraries, the museum of the earth, youth groups, and local 4-H groups. I have also assisted with outreach events organized by Cornell's Spacecraft and Planetary Imaging Facility (SPIF).

I am in my sixth semester of being a graduate TA, including my second year running a class of my own design. I adapted the UCF Astronomy Society's stratospheric balloon project into an optional one credit lab class for our intro to astronomy students.

In lab 1 the students propose designs for a weather balloon payload that fits within a $600 budget and 800g weight limit. The proposal includes constructing a prototype of the structure of the payload from old styrofoam containers and cardboard and writing a proposal for what electronics they want to use their budget on.

In lab 2 the lab groups negotiate these multiple proposals down to a single proposal within the timeframe of a single 2.5 hour lab session.

The third lab involves constructing and completing the payload, including soldering and programming the electronics, performing drop tests to determine the payload's terminal velocity, and learning to calculate predicted landing sites using a program that integrates high altitude wind profiles.

The fourth lab is launch and recovery of the weather balloon.

Occultation Observations of Saturn with *Cassini* VIMS

1. Goals of the Investigation

During *Cassini*'s 13 years in orbit around Saturn, the spacecraft's Visual and Infrared Mapping Spectrometer (VIMS) performed over 100 stellar occultation experiments on Saturn, covering a wide range of latitudes and seasons. Nicholson et al. (2018) describe the VIMS campaign of occultations, including the relevant instrumental setups for observing stellar and solar occultations, event predictions, geometric and photometric calibrations, and instrumental sensitivity.

Occultation observations at different observer geometries and wavelengths probe different levels of a planet's atmosphere. Spacecraft radio occultations are sensitive to differential refraction (Kliore et al. 2004), and probe the lower stratosphere and upper troposphere of Saturn at pressures of a few mbar to $\sim$ 1 bar (Lindal et al. 1985). Earth-based visible and near-infrared occultations of the outer planets are also sensitive to differential refraction and probe the upper stratosphere and mesosphere at pressures in the microbar range (**?**Elliot 1979; French et al. 1978). Spacecraft UV occultations ($\lambda < 150$ nm) are dominated by molecular and atomic absorption and probe the thermosphere of Saturn at pressures in the nanobar to ~ 1 μbar range (Broadfoot et al. 1981; Sandel et al. 1982; Smith et al. 1983).

This proposal deals with occultations observed by the *Cassini* VIMS instrument, which took time series of spectra with 20-40 ms sample rates at near-infrared wavelengths ($0.88-5.1$ μm in 256 spectral channels) as stars disappeared behind Saturn. These data cover an intermediate regime where some wavelengths are dominated by differential refraction and some by molecular absorption (methane and ethane). They span pressures from ~ 20 μbar to ~ 5 mbar, covering a large part of Saturn's stratosphere. See figure 1 for an example of what a VIMS occultation looks like.

Modeling the effects of differential refraction reveals the temperature profile of the atmosphere. Modeling the effects of molecular absorption reveals the composition. This data is the first that allows us to retrieve both simultaneously from the same *Cassini* dataset and in the same region of the atmosphere.

The principle goals of observing Saturn stellar occultations with VIMS were to obtain light curves that could be inverted to obtain temperature-pressure profiles of the planet's stratosphere, and to obtain vertical profiles of CH_4 abundance in the upper stratosphere with which to test photochemical and eddy-diffusion models such as those of Moses et al. (2000) and Moses and Greathouse (2005). Some preliminary results have been presented by Nicholson et al. (2006) and Banfield et al. (2011), but so far no comprehensive study has been completed or published.

I propose to perform just such a comprehensive study that will attempt to answer the questions outlined in the previous paragraph and to address the NASA Planetary Science Research Program SMD 2014 Science Plan top-level goal to:

"Advance the understanding of how the chemical and physical processes in the Solar System operate, interact and evolve."

More specifically, we will address the topic:

"Investigate the origins, evolution, and properties of the atmospheres of planetary bodies (including satellites, small bodies, and exoplanets)"

as well as

"Enhance the scientific return of NASA Planetary Science Division missions through the analysis of data collected

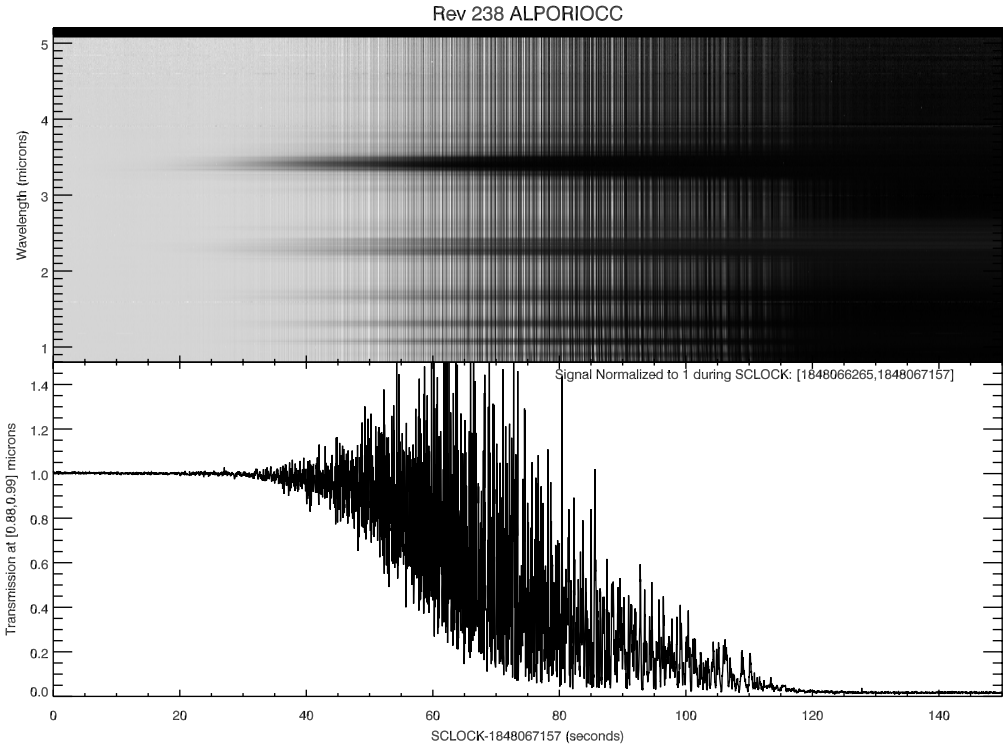

Fig. 1.— Occultation of α Orionis during Cassini rev: 238 at planetocentric latitude -64.9° from a range of $959,000$ km with an integration time of 20 ms.**Upper panel** shows stellar signal with wavelength increasing vertically and time increasing horizontally. Stellar signal drops due to differential refraction independently of wavelength except for the molecular absorption in the narrow horizontal bands at 3.4, 2.3, 1.7, 1.4, 1.1 and 0.9 μm. **The lower panel** shows the flux averaged between 0.9 and 1.0 μmwhere molecular extinction is unimportant. In both panels, the stellar flux is normalized to unity in the period prior to the occultation.

by those missions"

2. Scientific Significance

Pre-*Cassini* observations of Saturn's temperature show a peak in seasonal variation at around 3 mbar (Yanamandra-Fisher et al. 2005), the region that the VIMS stellar occultation data probe. CIRS observations by Flasar et al. (2004, 2005); Fletcher et al. (2007) confirm this. Our proposed analysis can provide far better altitude resolution than the CIRS results in this critical region. Furthermore, the CIRS results are derived from thermal emission in the methane band at 8μmand cannot easily disentangle variations in temperature from variations in methane mixing ratio. We expect methane abundances also to depend on latitude and season as described by Moses and Greathouse (2005) and Fouchet et al. (2009). The proposed analysis will allow us to recover temperature profiles and methane abundances *independently of each other* at various latitudes and at seasons spanning almost half of a Saturnian year. **(Science Project 1: Verify CIRS Results)**

The chemical abundance profiles calcu-

lated in Moses and Greathouse (2005) match the "methane cycle" described in D.F. Strobel (1969). Methane diffuses up through the stratosphere to the homopause, slowly dropping in abundance through the region of the stratosphere to which VIMS occultations are sensitive. Far above this region of the stratosphere, methane undergoes photodissociation and is converted to higher-order hydrocarbons which diffuse back down to the troposphere where they are converted back to methane. The gases diffuse from their source to their sink via turbulence- or wind-driven eddy diffusion. The rates of diffusion, production, and destruction of these gases determine the shape of the abundance profiles through the stratosphere seen in figure 2.

As noted by Fouchet et al. (2009), important byproducts of these multiple profiles will be a better determination of the altitude of the CH_4 homopause on Saturn (which is known to be quite variable with latitude from UV occultations Koskinen et al. 2013, 2015). This is a function of the rate of photochemistry, which destroys CH4 in the upper atmosphere (Fouchet et al. 2009), and the speed of zonal winds in the stratosphere which distort the shape of the planet through the centrifugal force (Merritt and Nicholson 2019). **(Science Project 2: Measure the Homopause)**

Photodissociated methane is partially converted into ethane on its way to becoming aerosols composed of higher order hydrocarbons. Chemical abundances in the stratosphere impact the thermal profile of the entire atmosphere since trace gasses are the major absorbers of radiation from the sun and Saturn's blackbody emissions from lower levels. The proposed analysis will constrain both the methane and ethane mixing ratios, giving us insight into seasonal variations in photochemistry and eddy-diffusion rates that we can compare to models such as those described in Moses and Greathouse (2005). **(Science Project 3: Test Models of Chemistry and Eddy-Diffusion)**

Photochemistry also leads to aerosol production. Although not very spectrally active in our observations, aerosols are thought to be chemically important as a factor in cloud formation because they sediment downwards to serve as cloud-condensation nuclei for condensible volatiles in the troposphere (Fletcher et al. 2018). We will constrain photochemistry and eddy-diffusion rates through a direct measurement of the relative mixing ratios of methane to ethane, which will help future investigators understand aerosol production in the thermosphere and cloud formation processes in the convective regions of the troposphere. We will measure these abundances with high radial resolution over the course of nearly half of a Saturnian year at a multitude of latitudes thanks to *Cassini*'s long-lasting mission in the Saturn system.

Finally, uncertainties in the production and optical properties of photochemical haze are a major stumbling blocks in current hot-Jupiter exoplanet atmospheric models and retrievals, as they are thought to be the cause of the flattening of the transit spectra of gaseous exoplanets (Fraine et al. 2013). Through providing a ground-truth understanding of the atmosphere of one of our local giant planets whose atmospheric chemistry is also photochemically driven, our analysis will help future studies constrain the atmospheres of these exciting bodies that we will soon be able to probe in greater detail with the James Webb Space Telescope, ELT-class ground-based telescopes, and other future telescopes.

3. Technical Background

3.1. Differential Refraction

Consider a light ray from the occulted star incident on a spherical planet of radius R, at an impact parameter ρ. As it penetrates more deeply into the atmosphere, where the refractive index of the gas is larger, the ray gradually refracts towards the planet's center until it reaches a minimum radius, after which it traces a mirror-

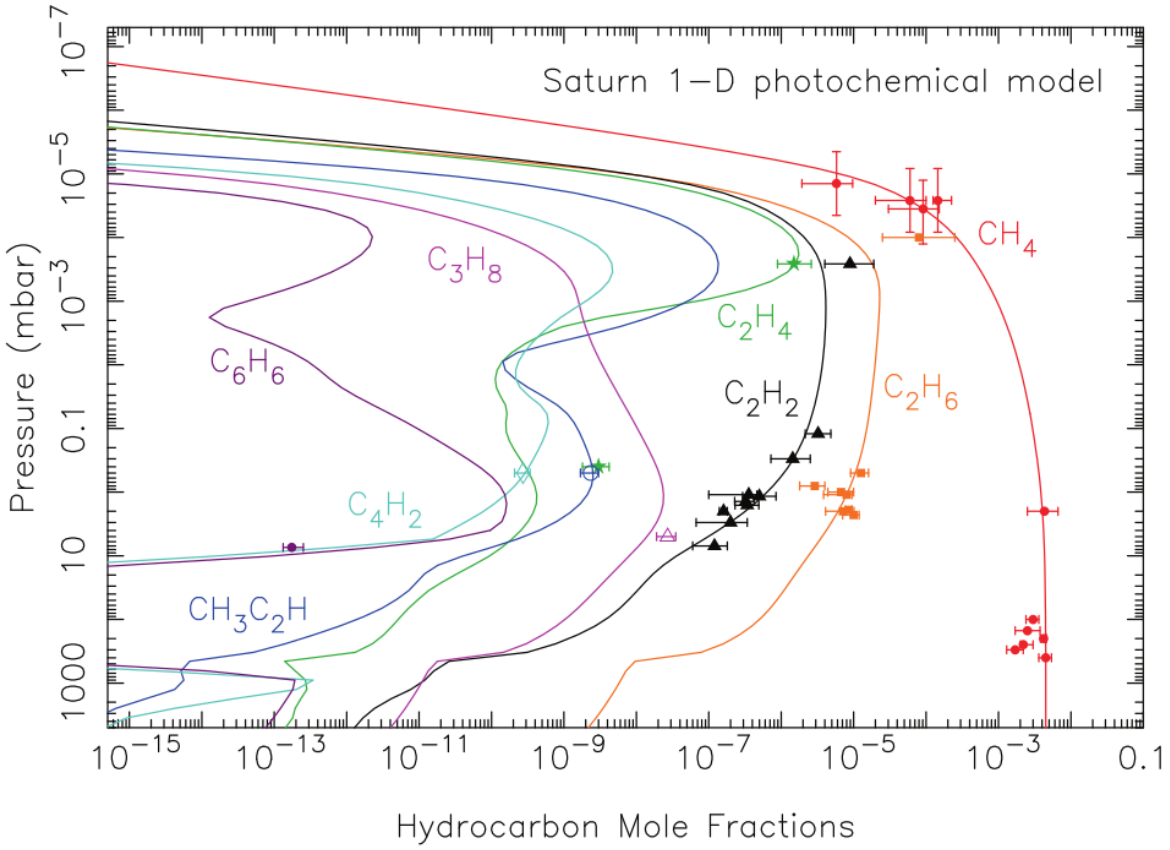

Fig. 2.— Figure taken from Fouchet et al. (2009). Hydrocarbon mole fractions as a function of pressure in Saturn's upper atmosphere as derived from the "Model C" 1-D steady-state photochemical model of Moses and Greathouse (2005). The solid curves represent the model profiles for the individual hydrocarbons (as labeled), and the symbols with associated error bars represent current infrared and ultraviolet observations. Methane is created in the troposphere and diffuses upwards to the homopause and the thermosphere where it is photochemically destroyed. Ethane and acetylene are produced at around $\times 10^{-4}$ mbar and diffuse down to the troposphere where they are converted back to methane. This is the methane cycle described in D.F. Strobel (1969)

image path back out of the atmosphere.

The formal expression for the overall angular deflection of the ray once it emerges from the atmosphere is:

$$\theta(\rho) = -2\rho \int_{r_0}^{\infty} \frac{dn/dr}{n\sqrt{n^2 r^2 - \rho^2}}\, dr, \qquad (1)$$

where $n(r)$ is the refractive index profile of the atmosphere, and the ray's minimum radius r_0 is specified by the condition $n(r_0)r_0 = \rho$.

Adjacent light rays are deflected by progressively larger amounts as ρ decreases and the rays penetrate more deeply into the atmosphere. As a result of this *differential refraction*, the flux of light from the source is reduced by a factor of Φ:

$$\Phi(\rho) = \left(1 - D\frac{d\theta}{d\rho}\right)^{-1} \left(1 - \frac{D\theta}{\rho}\right)^{-1}, \qquad (2)$$

where D is the distance from the planet to the observer. The second factor represents the focusing effect that occurs near the center of the geometric shadow and can be neglected for our data where $D\theta \ll \rho$.

As described in Elliot et al. (1977)

and French et al. (1978), we can use these two expressions to perform an inverse Abel transform and invert our occultation lightcurves in regions of the spectra dominated by differential refraction to acquire multiple radial profiles of the temperature and pressure in the planet's stratosphere.

This technique is standard for inversions of differential-refraction dominated stellar occultations. Due to Saturn's highly oblate shape, the above expressions are adjusted in practice to use a local spherical fit to the atmosphere.

We are confident that the attenuation of the starlight at wavelengths where hydrocarbon molecular absorption is negligible is dominated by the above-described impact of differential refraction and not aerosol-driven scattering extinction. Although aerosols are an important chemical component of Saturn's atmosphere, these particles are likely sub-micron in size and their scattering efficiency should decrease rapidly with decreasing wavelength, perhaps scaling as λ^{-q} where q is between 1 and 4. The aerosols on Titan follow such a power law with $q \simeq 1.8 \pm 0.5$ (Bellucci et al. 2009). The extinction in the VIMS Saturn occultations at wavelengths outside of the strong hydrocarbon bands is observed to be essentially *independent* of wavelength, strongly suggesting that aerosol extinction is negligible at the few mbar level and above and therefore we may neglect them in our models.

3.2. Morphology of an Occultation

Let's examine equation 2, neglect the second term, and substitute the appropriate isothermal expression for $\theta(\rho)$ to get an approximate expression of $\Phi(\rho)$ that can give us some intuition for how flux is lost over the course of an occultation:

$$\Phi(\rho) \simeq \left(1 + \frac{D\theta}{H}\right)^{-1}. \quad (3)$$

where the atmosphere's scale height $H = \mathcal{R}T/\mu g$, T is the temperature, μ is the mean molecular weight, g is the local gravitational acceleration, and $\mathcal{R}$ is the universal gas constant.

Note that $\Phi(\rho) \simeq \frac{1}{2}$ when $D\theta = H$, indicating that the impact parameter for which the flux from the source has halved is dependent on the distance to the observer D. This is the reason that Earth-based stellar occultations probe much higher atmospheric levels than do those observed by orbiting spacecraft at similar wavelengths. For typical VIMS Saturn occultations, the refractive half-light level is at $p \sim 3$ mbar, assuming that $\bar{T}_{stratosphere} \sim 140$K.

The bending angle θ scales with the refractivity at the point of deepest penetration of the ray which increases exponentially with depth, so the attenuation of the rays increases rapidly as they drop below the half-light level. However, the observed brightness of the occulted star falls off much more gradually because the light rays are also deflected further into the planet's geometric shadow, prolonging the star's visibility. The result is that such a purely-refractive lightcurve has a long tail that extends well beyond the half-light time. In our observations this tail is truncated because the image of the star is refracted out of the single 0.25×0.5 mrad VIMS pixel, leading to a "floor" beyond which we cannot probe. This occurs at $\Phi \simeq \frac{1}{3.5}$, for $\theta \simeq 0.25$ mrad, $D \simeq 5{\times}10^5$ km, and $H \simeq 50$ km. This is empirically confirmed by a small number of VIMS occultations observed in the instrument's imaging-mode, which has a larger field-of-view at the expense of less-frequent time-sampling.

3.3. Molecular Absorption

Let's consider an "onion-skin" model of an atmosphere for which each thin radial layer is of uniform composition and density. As a ray of star light passes through each of these layers, it is attenuated according to the equation:

$$\Phi(\lambda) = \Phi_0 \; e^{-\delta\tau(\lambda)}, \quad (4)$$

where Φ_0 is the attenuation experienced before entering that layer and $\delta\tau(\lambda)$ is the optical depth

of the layer as a function of wavelength, described by the equation:

$$\delta\tau(\lambda) = \kappa(\lambda)Ld \quad (5)$$

Here, κ is the absorption coefficient, L is the slant pathlength, and d is the density of the layer which is known from the inversion of the lightcurve at the refraction-dominated continuum wavelengths.

The data for a given occultation can be thought of as a time-series of spectra, each of which cuts a deeper path through the atmosphere than its predecessor. Each time-step can be used to constrain the opacity of an additional deeper layer, and then be used as an input to the next timestep since that layer will also be probed during the subsequent observations. Datapoints can be binned in time to increase signal to noise at the expense of the radial resolution of the resulting abundance profile. We call this technique "onion-peeling" and a preliminary proof-of-concept using a single wavelength bin was presented by Banfield et al. (2011).

We will fit a model to a full-spectrum $\kappa(\lambda)$ calculated in each layer from our data. A model spectrum will be calculated with a line-by-line approach using Voigt profiles calculated using the pressures and temperatures from our refraction inversions described above. We will use line list databases such as the HITEMP database from HITRAN [1] (Gordon et al. 2017) for each gas relevant to Saturn's atmosphere. The contributions of each gas (chiefly CH_4 and C_2H_6, but possibly also C_2H_2) to the final opacity are independent and proportional to their mixing ratios, which will be fit to the data.

In practice, hydrogen and helium are essentially transparent in the near-infrared for any reasonable path length through the stratosphere[2], so the opacity is dominated by trace gases, methane, ethane, and acetylene (Moses and Greathouse 2005).

4. Project Summary

Our project is to write a code that will calculate an onion-skin model of Saturn's stratosphere from the VIMS occultation data.

End of 2019 to Early 2020: We will first carry out an atmospheric inversion on the refraction-dominated parts of the occultation spectra to acquire the temperature, pressure, and density of each layer of the onion, at a radius accurately known from the occultation geometry.

Rest of 2020: We will then "peel" that onion to calculate molecular abundances in each layer as the occultation descends through Saturn's atmosphere. We will accomplish this by fitting spectra calculated to those observed over the course of the occultation.

This procedure will provide local atmospheric profiles on Saturn at each of the locations and times probed by an occultation.

2021: We will look for trends in latitude and season within this collection of profiles with three major publishable goals in mind:

1. Verify CIRS results
2. Measure CH_4 homopause
3. Constrain chemistry models and eddy-diffusion rates

2022: Publish papers and defend my thesis by mid-summer.

---

[1] https://hitran.org/hitemp

[2] H_2 does have a fundamental vibrational transition at 2.1 μm, which is detectable in the spectra of the Jovian planets, but this is a collision-induced absorption that scales as p^2, and so is very weak in the stratosphere, even for very long path lengths.

REFERENCES

Banfield, D., Gierasch, P. J., Conrath, B. J., Nicholson, P. D., Hedman, M. M. 2011. Saturn's He and CH4 Abundances from Cassini VIMS Occultations & CIRS Limb Spectra. EPSC-DPS Joint Meeting 2011 1548.

Bellucci, A., Sicardy, B., Drossart, P., Rannou, P., Nicholson, P. D., Hedman, M., Baines, K. H., Burrati, B. 2009. Titan solar occultation observed by Cassini/VIMS: Gas absorption and constraints on aerosol composition. Icarus 201, 198-216.

Broadfoot, A. L., and 15 colleagues 1981. Extreme ultraviolet observations from Voyager 1 encounter with Saturn. Science 212, 206-211.

Campo, C. J. and Harrington, J. and Hardy, R. A. and Stevenson, K. B. and Nymeyer, S. and Ragozzine, D. and Lust, N. B. and Anderson, D. R. and Collier-Cameron, A. and Blecic, J. and Britt, C. B. T. and Bowman, W. C. and Wheatley, P. J. and Loredo, T. J. and Deming, D. and Hebb, L. and Hellier, C. and Maxted, P. F. L. and Pollaco, D. and West, R. G. 2011. On the Orbit of Exoplanet WASP-12b The AstroPhysical Journal 727, 125

Cubillos, P. and Harrington, J. and Madhusudhan, N. and Foster, A. S. D. and Lust, N. B. and Hardy, R. A. and Bowman, M. O. 2014. A Spitzer Five-band Analysis of the Jupiter-sized Planet TrES-1 AstroPhysical Journal 797, 42.

Elliot, J. L., French, R. G., Dunham, E., Gierasch, P. J., Veverka, J., Church, C., Sagan, C. 1977. Occultation of Epsilon Geminorum by Mars. II - The structure and extinction of the Martian upper atmosphere. The Astrophysical Journal 217, 661-679.

Elliot, J. L. 1979. Stellar occultation studies of the solar system. Annual Review of Astronomy and Astrophysics 17, 445-475.

Flasar, F. M. and Kunde, V. G. and Abbas, M. M. and Achterberg, R. K. and Ade, P. and Barucci, A. and Bézard, B. and Bjoraker, G. L. and Brasunas, J. C. and Calcutt, S. and Carlson, R. and Césarsky, C. J. and Conrath, B. J. and Coradini, A. and Courtin, R. and Coustenis, A. and Edberg, S. and Edgington, S. and Ferrari, C. and Fouchet, T. and Gautier, D. and Gierasch, P. J. and Grossman, K. and Irwin, P. and Jennings, D. E. and Lellouch, E. and Mamoutkine, A. A. and Marten, A. and Meyer, J. P. and Nixon, C. A. and Orton, G. S. and Owen, T. C. and Pearl, J. C. and Prangé, R. and Raulin, F. and Read, P. L. and Romani, P. N. and Samuelson, R. E. and Segura, M. E. and Showalter, M. R. and Simon-Miller, A. A. and Smith, M. D. and Spencer, J. R. and Spilker, L. J. and Taylor, F. W., 2004. Exploring The Saturn System In The Thermal Infrared: The Composite Infrared Spectrometer Space Science Reviews Vol 115 Issue 1-4 pp169-297.

Flasar, F. M. and Achterberg, R. K. and Conrath, B. J. and Pearl, J. C. and Bjoraker, G. L. and Jennings, D. E. and Romani, P. N. and Simon-Miller, A. A. and Kunde, V. G. and Nixon, C. A. and Bézard, B. and Orton, G. S. and Spilker, L. J. and Spencer, J. R. and Irwin, P. G. J. and Teanby, N. A. and Owen, T. C. and Brasunas, J. and Segura, M. E. and Carlson, R. C. and Mamoutkine, A. and Gierasch, P. J. and Schinder, P. J. and Showalter,

M. R. and Ferrari, C. and Barucci, A. and Courtin, R. and Coustenis, A. and Fouchet, T. and Gautier, D. and Lellouch, E. and Marten, A. and Prangé, R. and Strobel, D. F. and Calcutt, S. B. and Read, P. L. and Taylor, F. W. and Bowles, N. and Samuelson, R. E. and Abbas, M. M. and Raulin, F. and Ade, P. and Edgington, S. and Pilorz, S. and Wallis, B. and Wishnow, 2005 Temperatures, Winds, and Composition in the Saturnian System Science 307, 1247-1251.

Fletcher, L. N. and Irwin, P. G. J. and Teanby, N. A. and Orton, G. S. and Parrish, P. D. and de Kok, R. and Howett, C. and Calcutt, S. B. and Bowles, N. and Taylor, F. W., 2007 Characterising Saturn's Vertical Temperature Structure from Cassini/CIRS Icarus 189, 457-478.

Fletcher, L. N. Greathouse, T. K. Guerlet, S. Moses, J. I. West, R. A. 2018 Saturn's Seasonally Changing Atmosphere Saturn in the 21st Century, 251-294.

Foster, A. S. D. Harrington, J. Cubillos, P. E. Blecic, J. Foster, A. J. Challener, R. C. Garland, J. DeLarme, E. Bakos, G. A. Hartman, J. D. The Atmosphere and Orbit of the Eccentric Hot Jupiter HAT-P-30b from Spitzer Eclipses 2019 ApJ, Submitted

Fouchet, T. and Moses, J. I. and Conrath, B. J. 2009. Saturn: Composition and Chemistry Saturn from Cassini-Huygens, 83-112.

Fraine, J. D. and Deming, D. and Gillon, M. and Jehin, E. and Demory, B.-O. and Benneke, B. and Seager, S. and Lewis, N. K. and Knutson, H. and Désert, J.-M. 2013. Spitzer Transits of the Super-Earth GJ1214b and Implications for its Atmosphere Astrophysical Journal 765, 127.

French, R. G., Elliot, J. L., Gierasch, P. J. 1978. Analysis of stellar occultation data - Effects of photon noise and initial conditions. Icarus 33, 186-202.

Gordon, I. E. Rothman, L. S. Hill, C. 2017. The HITRAN2016 Molecular Spectroscopic Database Journal of Quantitative Spectroscopy and Radiative Transfer 203, 3-69.

Harrington, J. Himes, M. D. Cubillos, P. E. Blecic, J. Rojo, P. M. Challener, R. C. Lust, N. B. Bowman, M. O. Blumenthal, S. D. Dobbs-Dixon, I. Foster, A. S. D. Foster, A. J. Green, M. R. Loredo, T. J. McIntyre, K. J. Stemm, M. M. 2019 An Open-Source Bayesian Atmospheric Radiative Transfer (BART) Code: 1. Design, Tests, and Application to Exoplanet HD 189733b ApJ, Submitted

Kliore, A. J., and 12 colleagues 2004. Cassini Radio Science. Space Science Reviews 115, 1-70.

Koskinen, T. T., Sandel, B. R., Yelle, R. V., Capalbo, F. J., Holsclaw, G. M., McClintock, W. E., Edgington, S. 2013. The density and temperature structure near the exobase of Saturn from Cassini UVIS solar occultations. Icarus 226, 1318-1330.

Koskinen, T. T., Sandel, B. R., Yelle, R. V., Strobel, D. F., Müller-Wodarg, I. C. F., Erwin, J. T. 2015. Saturn's variable thermosphere from Cassini/UVIS occultations. Icarus 260, 174-189.

Merritt, N. I. and Nicholson, P. D. 2019. Using Cassini VIMS Stellar Occultations to Investigate Geostrophic Winds in Saturn's Atmosphere. American Astronomical Society Meeting Abstracts 233, #255.10

Lindal, G. F., Sweetnam, D. N., Eshleman, V. R. 1985. The atmosphere of Saturn - an analysis of the Voyager radio occultation measurements. The Astronomical Journal 90, 1136-1146.

Maltagliati, L., Bézard, B., Vinatier, S., Hedman, M. M., Lellouch, E., Nicholson, P. D., Sotin, C., de Kok, R. J., Sicardy, B. 2015. Titan's atmosphere as observed by Cassini/VIMS solar occultations: CH_4, CO and evidence for C_2H_6 absorption. Icarus 248, 1-24.

Moses, J. I., Bézard, B., Lellouch, E., Gladstone, G. R., Feuchtgruber, H., Allen, M. 2000. Photochemistry of Saturn's Atmosphere. I. Hydrocarbon Chemistry and Comparisons with ISO Observations. Icarus 143, 244-298.

Moses, J. I., Greathouse, T. K. 2005. Latitudinal and seasonal models of stratospheric photochemistry on Saturn: Comparison with infrared data from IRTF/TEXES. Journal of Geophysical Research (Planets) 110, E09007.

Nicholson, P. D., Hedman, M. M., Gierasch, P. J., Cassini VIMS Team 2006. Probing Saturn's Atmosphere with Procyon. Bulletin of the American Astronomical Society 38, 39.06.

Nicholson, P. D., Hedman, M. M., Ansty, T. M., 2018. Occultation observations of Saturn's Rings with Cassini VIMS. (in preparation).

Rojo, P. M. 2006, PhD thesis, Cornell University

Sandel, B. R., and 12 colleagues 1982. Extreme ultraviolet observations from the Voyager 2 encounter with Saturn. Science 215, 548-553.

Smith, G. R., Shemansky, D. E., Holberg, J. B., Broadfoot, A. L., Sandel, B. R., McConnell, J. C. 1983. Saturn's upper atmosphere from the Voyager 2 EUV solar and stellar occultations. Journal of Geophysical Research 88, 8667-8678.

Stevenson, K. B. Stevenson, K. B. and Harrington, J. and Fortney, J. J. and Loredo, T. J. and Hardy, R. A. and Nymeyer, S. and Bowman, W. C. and Cubillos, P. and Bowman, M. O. and Hardin, M. 2012a Transit and Eclipse Analyses of the Exoplanet HD 149026b Using BLISS Mapping 2012a ApJ, 754, 136.

Strobel, D. F., 1969. The Photochemistry of Methane in the Jovian Atmosphere Journal of Atmospheric Sciences 26, 906-911.

Yanamandra-Fisher, P. A. and Orton, G. S. and Fisher, B. M. 2005. Mid-infrared spectrophotometry of Saturn's Ring System Highlights of Astronomy 13, 777.